Review

Impact Testing on the Pristine and Repaired Composite Materials for Aerostructures

Zoe E. C. Hall [1] , **Jun Liu** [1], **Richard A. Brooks** [1], **Haibao Liu** [2,*] **and John P. Dear** [1,*]

1   Department of Mechanical Engineering, Imperial College London, London SW7 2AZ, UK
2   Centre for Aeronautics, Cranfield University, Cranfield MK43 0AL, UK
*   Correspondence: haibao.liu@cranfield.ac.uk (H.L.); j.dear@imperial.ac.uk (J.P.D.)

Abstract: Aircraft technologies and materials have been developing and improving drastically over the last hundred years. Over the last three decades, an interest in the use of composites for external structures has become prominent. For this to be possible, thorough research on the performance of composite materials, specifically the impact performance, have been carried out. For example, research of impact testing for pristine carbon-reinforced epoxy composites mentions matrix cracks, fibre fracture, and delamination as the failure modes that require monitoring. In addition, thorough testing has been carried out on composites repaired with an adhesive bond to observe the effects of conditioning on the adhesively bonded repair. The results suggest there are no major changes in the adhesive under the testing condition. By reviewing the impact testing on the pristine and repaired composite materials for aerostructures, this paper aims to illustrate the main findings and also explore the potential future work in this research scope.

Keywords: carbon fibre reinforced polymer composites; impact testing; finite element analysis

1. Introduction

Materials for aerostructures require vigorous testing to ensure they can withstand the range of conditions an aircraft is exposed to. With areas such as static bending and free vibration response of materials for this application, including composite panels, having been widely investigated [1–5]. A specific area of interest is the impact performance of composite materials, including both soft and hard impacts. Hard impact conditions are experienced by an aircraft in many situations, for example when debris hits the structures. An impact is classified as hard if the impactor does not significantly deform upon initial impact. This type of interaction results in permanent indentation on the impacted surface of the composite laminates, whereas soft impacts do not leave any marks on the impacted surface. This is because the impactor deforms while impacting the sample, which causes a reduction in the stress concentration from the impact. Common examples of soft impacts that an aircraft would experience are bird strikes and hailstones. A further consideration is how to repair damaged composite components of aircraft structures. Currently, aluminium sections are repaired by bolting on a new piece of material to conceal the damage. However, this method is not suitable for composite materials, meaning thorough research is required to see what repair techniques can be used for composites.

This document is split into three main sections: the first discussing the research that has been carried out on impact testing of pristine composite materials; the second evaluating the research carried out on repairing damaged sections of composites; and the final assessing the numerical models developed for impact testing of both pristine and repaired composite structures.

2. Response of Pristine Composites under Impact Loading

2.1. Hard Impact

A large amount of research has been carried out in the area of hard impact testing of composite materials. There are low-, medium-, and high-velocity impacts, with the former two being discussed in this section. The velocity of the impact affects how much and what type of damage is observed. It is also known that, for hard impacts, the shape of the projectile greatly affects the failure mode of the composite and how much damage occurs.

2.1.1. Low Velocity

Liu et al. [6] carried out experimental and numerical studies on the impact response of damage-tolerant hybrid unidirectional and woven carbon-fibre reinforced composite laminates. Drop-weight impact testing, with a 12.7 mm diameter, steel, round-nosed impactor, was used to subject the specimens to the required conditions. Three impact energies were implemented, 10, 17, and 25 J, and after impact the panels were assessed using a c-scan system. In their research, Liu at al. [6] comment on the fact that carbon-fibre reinforced polymers demonstrate their superior properties in the fibre direction but have very low strength and fracture toughness in the through thickness direction. This means that low-velocity impact is a critical load case for composite aerostructures due to delamination and matrix cracks, which could significantly reduce the residual strength of composite structures. This insight shows that any potential material for the exterior of an aircraft requires thorough research into how it responds to hard- and low-velocity impacts. Liu et al. [6] concluded that the maximum reaction force and damage area were both linearly dependent on the impact energy. It was also found that the layup of the laminate changed the overall bending stiffness and, therefore, the overall impact response of the composite samples. The main failure mode detected in post-impacted composites was delamination, with minimal matrix cracking and no fibre breakage. Finally, Liu et al. [6] stated that using woven plies on the top and bottom layers of a sample can reduce the extent of damage from an impact. Although these conclusions are likely valid, there was variation in the values obtained in repeat specimens, up to $\pm 23.5\%$ in one case. This disparity could be due to outliers from set-up or measurement errors that could therefore be discounted, or some samples may deviate from the trends concluded above, potentially undermining the above findings.

Sjogren et al. [7] studied Hexcel HTA/6376C carbon-reinforced epoxy samples and tested them using a drop weight machine, to perform large mass, low-velocity impact tests. It was observed that fibre breakage was centred around the impact site and extended over roughly half the delamination area. This fibre breakage generally grew perpendicular to the fibre direction, but, when the fibre orientation between adjacent plies was less than $90°$, a mixture of fibre breakage growth perpendicular to the fibre direction and following the matrix cracks was seen. Samples of 16 and 48 plies were tested, with the former demonstrating a much larger quantity of fibre breakage. Measuring the elastic moduli in tension and compression, Sjogren et al. [7] concluded that the values of these moduli were largely dependent on the amount of fibre breakage. This meant that the 16-ply samples were seen to have a more significant decrease in elastic moduli, especially the elastic modulus in tension. However, the samples tested in this research were cut to be 180×180 mm^2, which does not meet the drop weight testing standard that suggests a size of 100×150 mm^2. It is likely that the overall conclusions from this work could be applied to carbon-fibre-reinforced polymer composites, but the specific values would most likely not be comparable to other testing in this area.

In continuation, for low-velocity impacts, Clark et al. [8] also used a drop weight testing machine, at a constant impact energy of 12.20 ± 0.09 J, to test the effect of low-velocity impacts on the fatigue life of aerostructures. Clark et al. [8] concluded that the low-level impact damage could propagate to failure due to compression-dominated fatigue and saw that damage growth rate depended on damage width. This demonstrates that impact damage is likely to lead to failure from fatigue if it does not fail immediately, meaning

considering how to repair or replace composite panels is of interest. As with the work of Sjogren et al. [7], it was observed that damage growth primarily occurred perpendicular to the direction of the fibres rather than along plies. Similarly to above, the panel size for impact tests did not meet the relevant standard, being $300 \times 100 \text{ mm}^2$, meaning that the specific damage area values cannot be compared to other work. Additionally, the damage areas found were not overly precise due to the technique implemented to calculate them using the deformation on the rear face to estimate the delamination damage throughout the panel. However, the conclusions are deemed relevant despite these limitations.

Topac et al. [9] impacted CFRP beams with the aim of determining the damage modes that occur throughout the impact event. For this reason, a blocked cross-ply lay-up was chosen. The panels were cut to give $100 \times 17 \times 4.8 \text{ mm}^3$ specimens, and a hole was drilled at each end to allow a screw to be placed through the clamps and specimens, so that slipping was prevented. Through c-scanning and optical microscopy, the samples were checked for damage from machining prior to any testing. The specimens were impacted at 7.7 J and evaluated using an optical microscope and DIC. The same damage path was observed in all samples, with a central delamination between the $0°/90°$ (upper) interface feeding into diagonal matrix cracks through the $90°$ layers leading to delaminations between the $90°/0°$ (lower) interface that extended outwards. In the cases where the impact damage was symmetrical around the centre of the specimen, matrix cracking initiated on one side before the other and, in some cases, two cracks initiated on one side at once. From the six samples tested, it was found that the average angle, location from the centre, and time of initiation of the first and second matrix crack were $49°$, 18.1 mm and 268 μs and $48°$, 16.3 mm and 650 μs, respectively. Finally, it was observed with a high-speed camera, that the matrix cracking initiates first and then leads to the two delaminations extending from both ends of the crack. Overall, this research gives invaluable information on how damage initiates and propagates through composite panels during an impact event.

Lastly, Ullah et al. [10] impacted specimens at a low velocity with a hard impactor, but, to subject the panel to bending, the lower part of the specimen was fixed in place, and the upper 30 mm was hit with the impactor in a pendulum motion. Pristine, damaged, and fractured woven CFRP samples were all tested. In the force time traces, the former two demonstrated smooth curves, whilst the latter saw a sudden load drop, which suggests damage initiated at this point in this sample. The results were compared to drop weight testing previously performed, and it was seen that the bending impact test resulted in failure at a lower impact energy. This highlights the importance of considering the type of impact and the boundary conditions of the component.

2.1.2. Intermediate Velocity

Research in this area has been carried out by Olsson [11] who considered low- and medium-velocity impacts as a cause of failure in polymer matrix composites. These velocities are defined as considerably less than 75 m/s, which is said to be the minimum velocity for penetration to occur and therefore is considered a high-velocity impact. Olsson [11] discussed different wave shapes that can occur from an impact: (a) fast tensile or compressive waves in the plane of the laminate; (b) fast surface waves along the laminate surface; (c) somewhat slower tensile or compressive waves through the thickness of the laminate; (d) relatively slow transient shear and flexural waves within the laminate; and (e) a slow oscillation involving a global quasi-static deflection mode. These wave shapes are shown in Figure 1 below.

It is noted that the third of these wave shapes, the through thickness wave, easily causes damage. This is said to be because it has a large amplitude and acts in a direction with low strength, but the influence of these waves is fairly local. Furthermore, it is stated that impact damage may reduce the strength and stability of composite structures significantly. Olsson [11] found the effect to be large in compression, with reductions of up to 70% from the undamaged strength being observed. From experimentation, it was concluded that the reduction in failure strain is smaller for tougher resins. However, the

toughest resin tested, PEEK, is not always chosen for aircraft structures. This means the reduction in failure strain that comes with increasing the brittleness of the resin should be considered when choosing a material.
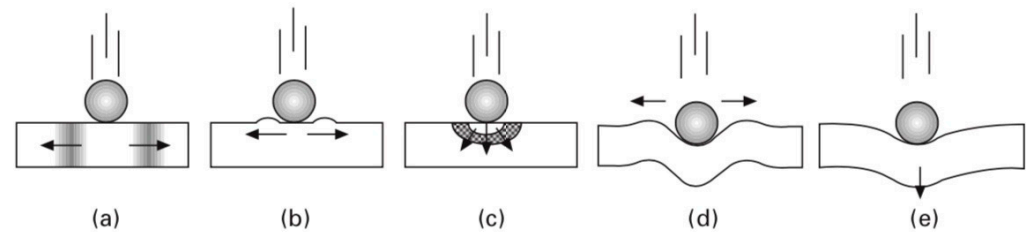

Figure 1. Wave shapes discussed by Olsson [11]: (**a**) fast tensile or compressive waves in the plane of the laminate, (**b**) fast surface waves along the laminate surface, (**c**) somewhat slower tensile or compressive waves through the thickness of the laminate, (**d**) relatively slow transient shear and flexural waves within the laminate, and (**e**) slow oscillation involving global quasi-static deflection.

2.2. Soft Impact

An important area of research for aircraft materials is their performance under soft impacts, an example of which is the repeated soft impact from the stairs, which allow passengers to exit the aircraft, being rolled into the side of the aircraft. A seal, often made from rubber, is attached to the edge of the stairs that come into contact with the aircraft fuselage to soften the impact. These stairs, and other ground control vehicles, are not always pushed up to the aircraft with care, which can introduce damage. This is especially critical to investigate for composite materials because the damage that could be caused is commonly found on the rear (internal) face of the panel, rather than the external face, and so would not be visible to aircraft technicians and airport staff. It is also important to note that the internal face is ordinarily covered by the cabin lining, meaning the damage would not be visible from inside the aircraft either. This means that the failure modes and defects in the structure may go unnoticed, causing large safety risks when flying.

Hou et al. [12] carried out soft impact testing at a high velocity using a 10 g gelatine projectile to replicate the characteristics of a bird strike on a plane. Velocities between 200 and 330 m/s, which were achieved with a gas gun, were used on different carbon-fibre-reinforced epoxy composite systems. To achieve these impacts, a sabot was used in conjuction with the projectile and was removed, through the use of a separation device, prior to impact. A mixture of unidirectional and woven lay-ups was tested, with all samples being 216×102 mm^2. Hou et al. [12] deduced that the AS4/PR520 woven sample had the best impact resistance, with a damage initiation velocity of 255 m/s. In contrast, the Toray T800H/3900_2 unidirectional sample performed the worst, with a damage initiation velocity of 200 m/s and failing completely above this velocity. This lay-up only had 15 plies, whereas all the other unidirectional samples tested had 21. In general, the woven samples were seen to have a higher impact resistance than the unidirectional samples. Hou et al. [12] theorised that this might be due to the fact that transverse matrix cracking is contained by fibres in the woven material. The unidirectional sample seen to have the best performance was CYTEC 5250-4/T800, with a damage initiation velocity of 238 m/s, which is 17 m/s lower than that of the woven sample with the best observed performance. It was concluded that fibres HTA, IMS, and T800H were less tough than T300, IM7, 1238, M18, and T800. Similarly for resins, resin 8551_7 and 3900_2 were said to be tougher than other resins. Using gelatine projectiles to replicate the impact event of a birdstrike is effective and essential to ensure repeatability. However, the lack of repeatability observed when testing with real birds means this method potentially oversimplifies the problem.

Another application of high velocity, soft impact testing is for investigating the aircraft's response to hailstones. This is considered soft impact because the deformation of the hailstone during impact is significant. Pernas-Sanchez et al. [13] carried out testing in this area using a gas gun to launch ice projectiles at unidirectional carbon/epoxy laminates at a

range of speeds from 50 to 250 m/s. The technique to produce the ice projectiles, which involved melting and refreezing a manufactured ice block, ensured no cracks were present in the projectiles. However, it also resulted in a microstructure different to that observed in hailstones. It is likely that this did not affect the results and conclusions drawn, but this is a potential limitation to this work. Due to the ice deforming around the sample, it was observed that there was no damage on the front face. Pernas-Sanchez et al. [13] saw delamination as the main damage mechanism that composite laminates exhibit. Two different thicknesses of composite panel were used, 4 and 6 mm, as well as two diameters of ice projectile, 40 and 50 mm. This experiment found that the delamination initiation velocities for the 6 mm thick sample were 212 and 188 m/s for the 40 and 50 mm diameter projectiles, respectively. These values were 172 and 153 m/s for the 4 mm thick sample. This implies that the critical velocity of a composite sample depends strongly on its thickness and the size of the projectile impacting it. Pernas-Sanchez et al. [13] also commented that the main damage observed was interlaminar damage, meaning that the delamination occurred before any visual damage to the sample. This supports the point that the research of soft impact damage is critical to composite aerostructures since the primary failure mechanism is inside the layers and so not visible to the human eye.

3. Performance of Repaired Composites Subjected to Impact Loading

Another area of interest when considering the impact performance of composite materials for aircraft is the impact performance of repaired composites. A common method to repair the damaged composites is adhesive repair, which can be in the form of a patch or scarf repair. For the former, a patch of pristine material is adhered over the damage, and, for the latter, the damage is removed and then replaced with a pristine frustrum that is adhered in place. The performance of the materials after repair is of great interest because the life of an aircraft is significantly longer than some of its components, meaning repair is critical. It is especially critical for composite materials because, as seen in previous sections, the residual strength of the material is significantly reduced after damage. To mitigate this drawback, adhesive repair can be used to increase the residual strength of the damaged composite laminates.

3.1. Adhesively Bonded Repair

There are various ways to repair a composite sample, with a scarf joint being one option. A selection of some of the joint options by Kimiaeifar et al. [14] is shown in Figure 2.

Reasoning for choosing scarfed joints over lap joints was discussed by Pinto et al. [15], who stated that scarf repairs reduce peel stresses due to not causing substantial bending. It was also commented that the tapering of the edges means that the shear stress distributions are more uniform along the bond for scarf joints.

Katnam et al. [16] summarised the scientific challenges and opportunities of implementing adhesively bonded repairs of composite aerostructures. Scarf repair is preferable due to providing enhanced stress transfer mechanisms and joint efficiencies, as well as having a minimal impact on the aerodynamic properties of the aircraft. A drawback to this technique is that accurate material removal is required, meaning controlled composite machining processes must be used as conventional machining techniques can cause material damage from the force and heat generation. Furthermore, surface preparation is critical for adhesive joints so as not to reduce the efficiency of the repair. An automated process for this is preferable as it is more likely to produce a uniform and consistent surface than doing the preparation by hand. In general, it is commented that automating of various processes in this repair technique offers opportunities to improve the performance and repeatability of the joints.

To reduce the effects caused by conventional machining techniques, a possible alternative method is water jet cutting. Demiral et al. [17] assessed the damage to a CFRP cross-ply laminate that this technique can cause. The settings used on the water jet machine displayed a mean diameter of 0.76 mm, and the water pressure and jet angle were adjusted,

with values of 200 and 400 MPa and 0° and 30°, respectively. To assess the damage after cutting, scanning electron microscopy was used. Increasing the pressure resulted in more significant fibre damage. Increasing the cutting angle gave more fibre pull-out in the 90° cross-ply layers. These results suggest that a lower pressure and a shallower angle are preferable, although damage will still likely be incurred from the cutting method.
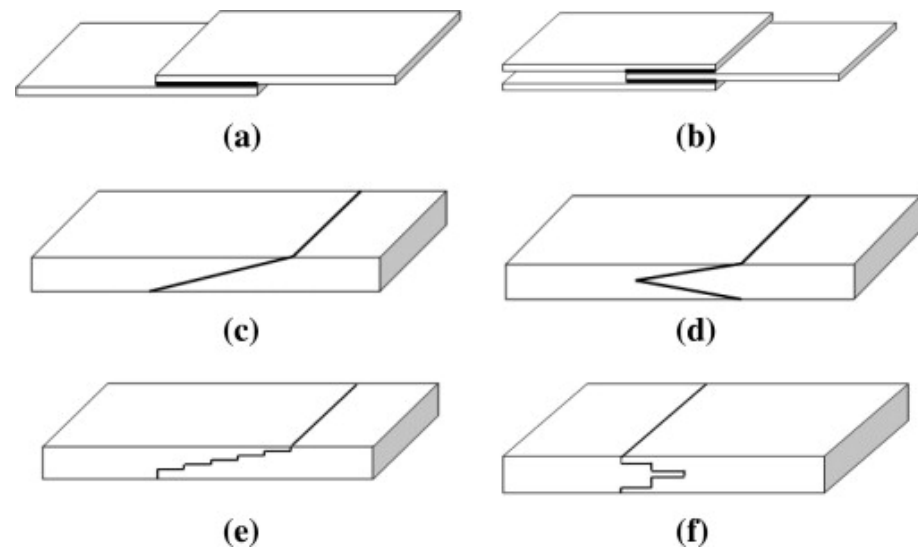

Figure 2. Types of adhesive joints shown by Kiniaeifar et al. [14]: (**a**) single lap joint, (**b**) double lap joint, (**c**) scarfed lap joint, (**d**) double sided scarfed joint, (**e**) stepped lap joint, and (**f**) double sided stepped lap joint.

Another potential challenge of scarf repair joints is aeration in the adhesive, causing voids that reduce the tensile strength recovery of the sample. Preau et al. [18] investigated this phenomenon and concluded that there was an average linear reduction in strength recovery of 4.5% per 1% void content by area in the adhesive. The void content was also said to influence the failure mode, with the more porous adhesive joints failing from cohesive failure in comparison to tensile failure for the void-free joints. This suggests that investigating how to reduce the quantity of voids in the adhesive layer would be beneficial to the performance of the final repaired material.

3.2. Tensile Testing

Charalambides et al. [19] performed static, fatigue, residual stress, adhesive tensile, and adhesive shear testing on repair joints. Additionally, they performed composite coupon, static, and fatigue testing on pristine panels. Static testing was performed using an Instron testing machine with a constant crosshead rate of 2 mm/min; fatigue tests were performed using a Mayes servo-hydraulic fatigue machine. Residual strength was tested by first performing fatigue testing and then static testing. Lastly, for the tensile and shear adhesive testing, the Instron testing machine was used with crosshead rates of 1 mm/min and 0.5 mm/min, respectively. All the testing was carried out on carbon-fibre-reinforced epoxy repair joints that were immersed in distilled water at 50 °C for periods up to 16 months. The effect of this treatment on the static and fatigue strengths was evaluated using the testing methods mentioned above. It was seen that there was no major effect on the static strengths of the repair joints, although the failure modes did change. However, this treatment is likely to have lowered the glass transition temperature, and so testing nearer that value would probably cause the static strengths to vary.

Kumar et al. [20] exclusively investigated the tensile failure of repaired carbon-fibre-reinforced epoxy repaired samples. Panels of $300 \times 300 \times 2$ mm^3 were hand laid and cured in a vacuum chamber and then cut down to give the required sample dimensions of $230 \times 12.5 \times 2$ mm^3. These samples were tested on an Instron testing machine at a

crosshead speed of 2.5 mm/min. Aluminium end tabs were bonded to the ends of the samples to ensure a secure grip and prevent local damage in the composite. Basically, two failure modes were observed: fibre fracture and pull-out, and cohesive shear failure of the adhesive film. The former occurred at a scarf angle less than 2°, and the latter occurred at an angle greater than 2°. It was also recorded that the largest scarf angle gave the most significant reduction in tensile strength. These results suggest that the tensile strength of the repaired composite is dependent on the scarf angle. As discussed by Katnam et al. [16], the employed samples required surface preparation to ensure the adhesive bonded successfully with the composite. This was achieved by Kumar et al. [20] by cleaning the surfaces with acetone to remove any debris from the machining process. This testing and the conclusions drawn appear to be valid; however, there is shown to be a large amount of variation between the stress–strain response for repeats of the same testing case.

Li et al. [21] compared the tensile performance of scarf repair joints with both single- and double-lap joints. The samples were manufactured to be 170×25 mm^2 and E-glass fibre-reinforced polymer end-tabs were added to make all the samples the same width at the ends for clamping. A number of repair variables were adjusted as part of the testing. For the scarf joints, the effect of adherend thickness and scarf angle were considered, and, for the lap joints, the effect of overlap length, adherend thickness, and adherend width were considered. It was found that the scarf joints had the greatest lap shear strength and strength-to-weight ratio out of all three joint types. Just looking at the scarf joints, the results imply that a smaller scarf angle gives a larger ultimate failure load but a decrease in lap shear strength. However, the relationship between scarf angle and lap shear strength plateaued beyond 8.13°, meaning that increasing beyond this will reduce the ultimate failure load whilst not improving the lap shear strength any further. It was also concluded that the increase in the adherend thickness gave a higher stiffness. For the lap joints, as the overlap length increased, the stiffness increased, and the failure mode transitioned from purely adhesive shear to purely delamination. Additionally, increasing the adherend thickness also increased the effective stiffness of the joint but resulted in a transition from purely delamination to a combination of delamination and adhesive shear. Lastly, the effect of the adherend width was similar to that of the adherend thickness.

Slattery et al. [22] carried out four-point-bending and tensile testing on pristine, damaged, and adhesively repaired panels to compare their flexural and tensile strengths. Specimens were repaired by drilling inlet holes in a damaged sample and injecting resin using a pump to form a vacuum. For the tensile testing, a servo-hydraulic testing machine was used with a crosshead speed of 0.02 mm/s. A similar machine was used for the four-point-bending testing, with a crosshead speed of 0.1 mm/s and the addition of a four-point-bending fixture. The fixture had a support span and load span of 300 and 150 mm, respectively. From the tensile testing, it was seen that the damaged sample had an ultimate tensile strength of 50.8%, and the value of the pristine sample and the repair raised this value to 53.5%, showing minimal improvement. The stress in the outer fibre was calculated in both tension and compression using the four-point-bending test. The damaged panel had values of 80.6% and 83.8% for the pristine sample for tension and compression, respectively. This was improved to 102.6% and 99.7% for the repaired sample in tension and compression, respectively, showing a more significant improvement than the tensile strength. Overall, the repair improved the mechanical properties of the damaged composite, with a more noticeable improvement in the flexural strength, demonstrating the benefits of the repair. Although the findings of this research are likely still valid, there is no mention of repeats, which is a potential flaw.

3.3. Impact Testing

3.3.1. Scarf Repairs under Low-Velocity Impacts

Liu et al. [23] used a drop test machine with a 16 mm diameter impactor to investigate how the repaired composite material would respond to impact. The samples were first impacted and then tested under tension, meaning the dimensions chosen were

$300 \times 50 \times 4$ mm^3 to ensure suitability for the latter. Focusing on the impact testing, a critical impact energy of 23 J was found, above which adhesive damage occurred and below which composite delamination and matrix cracking was the failure mode. This suggests that, below a specific impact energy, the repaired joint behaves similar to a pristine sample in terms of the failure modes that are present. Liu et al. [23] also state that the adhesive damage occurs at the scarf feathered tip of the back face, implying that this is the most easily broken area on the repaired joint.

Low-velocity impacts were performed on scarf-repaired CFRP composites by Liu et al. [24] using a drop weight machine. The samples tested were $250 \times 25 \times 6$ mm^3, with the stepped repair spanning 90 mm over the 100 mm cut-out window of the impact set up. Later, after testing, the panels were cut along the central line and assessed using optical microscopy. Impact energies of 3, 4, 5, 6, 8, and 10 J were used, with an energy above 4 J causing damage along the adhesive line. The adhesive damage occurred within steps one to five, which were subjected to tensile forces in addition to the shear forces throughout the material. Contrastingly, steps six to ten had little to no adhesive damage due to experiencing compressive forces that did not aid in the progression of the adhesive failure. Figure 3 below demonstrates where the adhesive damage occurred after undergoing a 10 J impact. Two main observations from the experimentation were commented on. Firstly, the adhesive failure from the impacts reduces the residual strength of the material, since the ability to withstand tensile forces is greatly reduced. Secondly, delamination of the composite itself initiates before the adhesive cracking and progresses at a slow rate through the material.
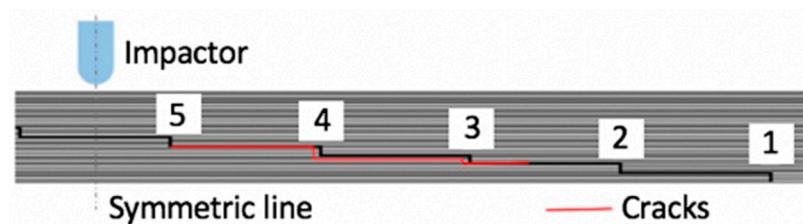

Figure 3. Location of cracks from 10 J impact performed by Liu et al. [24].

Atas et al. [25] also conducted some low-velocity impact testing but to compare two techniques of performing this type of repair: vacuum-assisted resin infusion process and hand lay-up technique. Samples were manufactured to be 100×100 mm^2, which does not adhere with the standard for drop weight testing, meaning the specific data obtained from this testing is most likely not comparable with other research in this area, although the general trends appear to still apply. Undamaged samples were tested using a drop weight testing machine alongside both repair types to allow a comparison. At low impact energies, the samples repaired using the hand lay-up process were seen to have a lower bending stiffness than those repaired with the infusion technique. Contrastingly, at higher impact energies both techniques had a similar performance. When comparing the pristine and repaired samples, it was seen that the former experienced damage formation in the fibre direction while the latter primarily failed along the repair line. Furthermore, the perforation energy for the pristine sample was around 30 J higher than that of both repair types.

Considering how pristine and scarf-joined composites perform under impact when subjected to a tensile preload, Li et al. [26] impacted prestrained CFRP composites. The scarf samples tested had a scarf angle of 5°, with all samples being impacted at 14.5 J over the cut-out window of 140×100 mm^2. The pristine samples were deemed to be unaffected by the pre-strain, with the impact damage area remaining more or less unchanged for all values of pre-strain. However, the repaired samples were seen to be sensitive to the pre-strain and unpredictable. For example, two specimens loaded at 3000 $\mu\varepsilon$ and impacted with projectile momentum values of 2.62 and 2.80 kg m/s failed entirely differently, with the former failing catastrophically and the latter suffering minor damage [26,27]. In general, it was found that the impact tolerance of the scarf joint was lower than that of the pristine material [26,27]. Herszberg et al. [27] theorised that there are two failure events, with a

weak connection between them, that occur during the catastrophic failure, the first being crushing and delamination, from the strains through the material thickness, and the second being vibration throughout the sample. Within the range of pre-strain values tested, it is the vibration mode that could cause failure of the repaired sample, with this value being dependent on the impact momentum rather than the impact energy. One of the main drawbacks of this research is that the method of impact testing resulted in a different impact velocity each time, meaning some general comparisons can be made, but a higher repeatability would be required to ensure comparability between specimens.

Liu et al. [28] also carried out low-velocity impact testing of scarf-repaired composites, considering the impact energy and impact location. Samples of $100 \times 150 \times 2.7$ mm^3 were repaired with frustrum that had a scarf angle of 6° and a lower diameter of 10 mm. It was observed that a larger damage area was produced when the impact was applied to the connection point between the parent and repair piece and also when a larger impact energy was used. This implies that the weakest part of the repaired composite is the join itself and that this is the area with the lowest residual strength.

3.3.2. Patch Repairs under Low-Velocity Impacts

Tie et al. [29] tested the performance of single-side patched repairs on CFRP composites, looking at different patch shapes and sizes. Each sample was $100 \times 150 \times 3.6$ mm^2. The testing had three stages: cutting out 3 mm radius holes from the parent material to represent damage; adhering either a circular or hexagonal patch; and using a drop weight machine to impact the sample. The radius of the circular patch was double the side length of the hexagonal patch, which had a value of 3.30 mm. This impact was located in line with, but not directly above, the damage area since the repair was located 20 mm from the centre of the sample. It was found that the circular patch had a smaller delamination surface area, with a value of 558 mm^2 in comparison to 572 mm^2 for the hexagonal patch repair. This implies that a circular patch is more effective at reducing the damage due to impact. Although this work offers some interesting conclusions, the material removal having a radius of 3 mm does not appear to come from any prior testing to ensure this area would cover the damage being simulated. Additionally, only two cases have been considered, and the difference in damage area is relatively minimal. Even though the findings appear acceptable, since repeats are also not explicitly mentioned, this highlights a potential flaw in the research.

Coelho et al. [30] performed impact tests on single- and double-patch-repaired composites to allow a comparison to be made between the two configurations. The composite used was a glass-fibre-reinforced epoxy, and 20 mm diameter holes were cut from the $100 \times 100 \times 3$ mm^3 samples to emulate damage. The hole was filled with an epoxy resin that was enhanced with nanoclays, and the patches, of 40×40 mm^2, were then adhered to the surface. Drop weight testing was performed on the samples, with an impactor of 10 mm diameter over a 75×75 mm^2 cut-out window. The single-patch repairs were impacted from 2 to 6 J, and the double-patch repairs from 6 to 12 J. It was observed that the double patch can withstand higher loads, with a load value of 97.1% higher than the single patch at an impact energy of 6 J. Furthermore, the double patch had an elastic energy that was higher by 51.2% at that same impact energy and also had a maximum displacement value of ca. 50% less than that of the single patch. These results imply that the double patch is not only superior but significantly so, due to its higher stiffness and therefore its higher impact fatigue life. Due to the impact energies chosen, the only value at which the two repair configurations could be compared was 6 J. Comparing at different energies could lead to different findings.

The effect of the impact location was also considered by Hou et al. [31], who tested the low-velocity impact performance of patch-repaired CFRP composites. Holes with a radius of 3 mm were cut in the $100 \times 150 \times 3.6$ mm^3 samples to represent damage, with the centre of the hole being either 20 or 30 mm from the centre of the sample. The holes were filled with an adhesive film, and then a circular patch, with a radius twice that of the hole, was

adhered on one side of the damage. It was seen that the peak impact force and delamination area for the 20 mm distance impact were 6124.2 N and 558 mm^2, respectively. These can then be compared to values of 6288.3 N and 536 mm^2 for the 30 mm distance impact. This suggests that impacting further from the repair results in less damage. However, both distances have relatively similar values, and so no clear conclusions can be drawn from only two distances having been tested.

3.3.3. High-Velocity Impacts

Kim et al. [32] performed high-velocity testing on pristine CFRP composite laminates and those with a scarf joint. A $100 \times 140 \times 3.2$ mm^3 sample with $5°$ scarf angle at the joint was impacted centrally and compared to a pristine sample of the same dimensions. The materials were subjected to pre-strain values of up to 5000 $\mu\varepsilon$ to see how this would affect the performance of each under impact conditions. The results showed that, for an impact energy of 8 J, the delamination area of pristine samples was generally unaffected. Contrastingly, the scarf joints experienced an increase in damage area when the in-plane loading was higher. This damage consisted of adhesive damage as well as the delaminations seen in the pristine samples. These results imply that the scarf joints perform in an inferior manner in comparison to the pristine samples.

Glass-fibre-reinforced epoxy was repaired with the scarf technique, and a patch was adhered to the top surface by Balaganesan et al. [33] who then performed high-velocity impact testing. A damaged sample was repaired by removing the damage layer by layer, increasing in diameter, and then applying epoxy to the bond-line and between plies as each new layer was applied one by one. These repairs were then tested using a gas gun and a round-nosed, steel projectile. Various different impact sites were tested for the repaired samples: on the patch centre and then 5, 10, 15, and 20 mm offset from the centre. In comparison to a pristine sample, it was observed that the energy absorbed during the impact decreased as the impact site moved away from the patch centre up to 15 mm offset. At the 20 mm offset, this value began to increase again. This suggests that this offset is far enough away from the repair for the performance to be similar to that of the undamaged composite. Furthermore, the delamination area on the rear face was highest for the pristine sample at 1600 mm^2, and the values for 0, 5, 10, 15, and 20 mm offsets were 0, 0, 192, 857, and 947 mm^2, respectively. This shows that the delamination area is greatly affected by repair and location of impact, with the area for the pristine sample having a value of around 1.7 times the largest delamination area of a repaired composite. Although the findings from this work appear reasonable, there is no explicit mention of repeat testing. Therefore, the reproducibility of this work is unknown.

4. Numerical Simulation

4.1. Modelling Impact of Pristine Composites

4.1.1. Hard Impact

Clark [34] investigated the areas in a sample in which delamination occurs in a composite laminate and the delamination growth under fatigue. This model was produced using the research and experimentation carried out by Clark et al. [8] and aimed to predict the delamination and cracking distribution within an impact damage zone. Clark [34] states that, from the model, it is implied that delamination would be more likely to occur in the region away from the impact centre line in the direction of the lower ply. It is commented that there is substantial agreement seen between the experimental results and those produced by the model for a 56-ply sample as well as a 20-ply sample. When using the model for a 10-ply laminate, Clark [34] describes the agreement as excellent. However, for a 24-ply laminate, some additional delamination development in another direction was seen in the experimental results in comparison to the model's prediction. It is speculated that this could be due to the effect of fatigue cycling or nearby plies influencing the result. The theory used to predict the delamination directions is valid, but this is a relatively simple model and so does not include any complex damage mechanisms, which is likely why the

predictions are not always accurate. Overall, the idea that the impact damage will spread in line with the fibre direction of the bottom ply at each interface is a fair assumption.

Topac et al. [9] implemented a LaRC04 failure criterion in conjunction with a cohesive zone model to numerically predict the initiation and evolution of damage modes in CFRP panels under impact loading conditions. When comparing to the experimental results discussed in Section 2.1.1, the model correctly predicted matrix cracking initiating first, leading to delaminations and, ultimately, the failure of the panel. However, experimentally, it was observed that the matrix cracks on each side of the panel initiated at different times. However, in the model, it was seen that the cracks initiated simultaneously, and the entire damage propagation process was completed after 274 µs, where the second matrix crack only initiated after 650 µs on average experimentally. This suggests that, although a model is successful at predicting the type of failure, the sequence of the damage modes and the timing may not align with those observed in experimental work.

Ullah et al. [10] implemented cohesive zone modelling for both the inter- and intralaminar damage within CFRP panels impacted by a pendulum. In general, the force time traces were predicted successfully, but the peak load was overpredicted in each case. However, the model was relatively simple and did not account for matrix cracking, meaning that the cross-section images produced by the model differed significantly from those obtained experimentally. Although this was the case, the length and distribution of delaminations through the panel in the cross-sections predicted by the model have relatively good agreement with those seen experimentally. This suggests that the simplification of implementing cohesive zone modelling for all damage mechanisms is potentially a suitable modelling method, especially as it saves on computational time in comparison to implementing a continuum-dynamics modelling approach for the intralaminar damage.

In hard impact testing, contrastingly to soft impact testing, indentation is often visible on the external face. Bouvet et al. [35] attempted to model the impact and the permanent indentation left after. This indentation was simulated with a plastic-like model based on experimental observations that showed matrix crack debris blocking a crack closure. For this reason, this plastic-like model was designed to take into account this debris and its effects on the indentation. Bouvet et al. [35] found a good correlation between impact force versus time and displacement using this model as well as significant similarities between the delaminated interfaces obtained experimentally and numerically. These results led to the conclusion that this modelling technique yields successful results, but the mesh sensitivity and other testing conditions should be simulated to further test the model.

Iannucci [36] modelled thin woven carbon composites under impact loading by controlling the energy dissipation per second, rather than the damage. At the time this model was produced, it was said that there were four approaches for damage in composite structures: failure criteria, fracture mechanics, plasticity, and damage mechanics, the latter of which is what this model is described as. Iannucci [36] states that the model can predict fibre fracture in both the weft and warp fibre bundles as well as fibre matrix deterioration. Implementing this for simulations gave final energy dissipated values that suggest good agreement between the experimentation and the simulation. However, issues of stability and localisation due to the included rate dependency required further investigation. Iannucci et al. [37] continued research in this area by investigating a damage mechanics approach to modelling the damage in composite structures using two constants. These constants were a stress threshold for damage and a critical energy release rate, which is specific to the delamination mode. Iannucci et al. [37] also claim that an explicit technique to maintain the energy dissipation independent of element size was not previously implemented but is in this new development of the model. The numerical modelling results compared with those from experiments is discussed by Iannucci et al. [38] who state that there is good agreement between these two results. It is also discussed that determining the value of various material constants, such as the intralaminar energies, requires further investigation. Although the model reliably predicts the onset of damage, an accurate determination of the energy dissipation is required for these predictions to actually be

reliable. Overall, the model relies on a number of constants and relationships being derived extremely accurately to give suitable results.

Xin et al. [39] proposed a progressive damage model to predict the performance of fibre-reinforced polymer composites under impact. The model is described as having three elements: quadratic stress-based failure criteria to predict the onset of failure; a combination of a linear form damage evolution law and the fracture energy approach to model the post-damage softening process; and the strain rate dependency of strength and modulus are taken into consideration. A number of failure modes are accounted for in this model, including matrix fracture, fibre breakage, and delamination. This model considered both in-plane and out-of-plane stresses. At the time this model was developed, other continuum damage mechanics models only catered for the effect the in-plane stresses had on the matrix and fibre failure modes, thus, ignoring out-of-plane stresses and their effect on the results. The model was said to be in good agreement with the experimental data, and it is commented that the fracture energy approach can be seen to reduce the mesh dependency.

Fibre-reinforced composite laminates were also considered by Ansari et al. [40] who performed a numerical investigation into the penetration and perforation behaviour of the composites under impact. There were four main conclusions from the modelling. Firstly, the damage in the composite plate and the ease of penetration of the projectile are both reduced with the employment of a fully restrained boundary condition. Secondly, for high-velocity impacts, the damage is primarily located near the impact site, and thinner samples had a smaller damage area. Thirdly, the length of the composite plate was seen to have an inversely proportional relationship to the ballistic limit velocity. Lastly, there was good agreement with the experimental data from the literature. However, the criteria used to determine interlaminar damage is not explicitly stated, potentially highlighting a limitation in this work and undermining the conclusions drawn.

Pham et al. [41] considered the low-velocity impact response of fibre-reinforced composite materials, as well as the compression after impact failure, using an enhanced continuum damage model that incorporated a 3D maximum stress criterion and then a fracture-energy-based smeared crack model. The model was verified to be in good agreement with experimental data from static open-hole tensile testing. Then, the interaction between delaminations and matrix cracking was investigated, and the model was used to see how these failure modes would affect the compressive strength after impact. The results of this research were, firstly, that the compressive strength is affected by the delaminations caused from impact. Secondly, the model is successful at giving information about impact and post-impact performance of the composite materials, as well as the damage that results from the impact event, quickly and efficiently.

4.1.2. Soft Impact

Due to the debris cloud and large amounts of deformation observed in the projectiles in soft impact testing, modelling this type of impact poses a number of difficulties. To simulate soft impacts such as bird strikes or hail stones that are highly deformable, Johnson et al. [42] used the Smooth Particle Hydrodynamics (SPH) method. This works by replacing the finite element mesh with interacting particles. So that this method simulated the impact accurately, pressure pulses measured from experimental testing were used to calibrate the gelatine material properties. Since in experimental results it was seen that both delamination and ply failures are of importance, Johnson et al. [42] developed a model including ply damage and interply delamination to predict the impact damage. It was concluded that further development is needed in the simulation of soft impacts, but the results seen using this model were described as encouraging. To further this research, Johnson et al. [43] implemented the model for two different soft impact cases, bird strikes and hailstones, and found good agreement in both cases.

Nishikawa et al. [44] also simulated the material response to high-velocity, soft impacts, but specifically modelled composite fan blades. Unidirectional carbon-fibre-reinforced polymer composites were of interest since they have been more widely used in fan blades

over recent years. The model used, when being verified, gave a maximum force value greater than that observed in experimental testing, but otherwise gave good agreement. The model was then used to investigate bird strike impacts on composite fan blades, with the results implying that the main factor controlling the ballistic limit is how the fibre-breakage mode occurs. Nishikawa et al. [44] concluded that this result suggests that using a simple unidirectional ply is useful for obtaining a first approximation for the ballistic limit. The simulated damage initiation also gave results that increasing the velocity of the projectile causes the failure to transition from a matrix-cracking mode to matrix-crushing and fibre-breaking modes. Nishikawa et al. [44] concluded that their simulation allows the ballistic limit to be analysed as a function of the material properties of the composite blade, unlike other models. However, this model does not account for interlaminar damage, which is potentially the cause of the disparity between numerical and experimental results. This means that the conclusions drawn may be flawed, although the extent to which this oversight affects the results is unknown.

Nishikawa et al. [44] mentioned that the boundary conditions being ambiguous could have caused the difference in maximum force value between their simulation and the experimental testing results. Li et al. [45] modelled two different boundary conditions, simply supported and clamped, to investigate the effect on the amount of delamination observed. The results found suggest that the effect of the boundary conditions on the maximum impact force is minimal, with only small plate lengths showing any variation in the result for different boundary conditions. When small plates were used, a slight increase in the maximum impact force was observed for the clamped boundary condition in relation to the simply supported boundary condition. This implies that Nishikawa et al. [44] having ambiguous boundary conditions is not likely to have had a significant impact on the overall result found. However, the model by Li et al. [45] considered a hard impact event, so there is potential that the boundary conditions would be affected when the impactor is soft.

In continuation, considering the modelling of soft impacts, Liu et al. [46] used experimental work, prior to performing numerical modelling, to determine the characteristics of a soft projectile during high-velocity impact. It was found that the soft projectile behaves as a viscoelastic-plastic fluid. From this finding, there was more of understanding of how the projectile interacts with the composite panel leading to the use of the SPH modelling technique, allowing the deformation of the soft projectile to be modelled successfully. To model the damage initiation in the panel, tensile and compressive fibre and matrix failure were all considered using Hashin's approach. Comparing the modelling results to those seen in the experimental work, good agreement was found. This same model was used in further simulations by Liu et al. [47], and good agreement was seen, but the model predicted values slightly lower than that seen experimentally, which is commented to be likely due to the composite panel being woven and the curvature effects that come with this.

Lastly, Liu at al. [48] used the same model to consider both hard and soft high-velocity impacts to consider the effect of the projectile hardness on the impact response of the composite. Since the two types of projectiles behave differently upon impact, it was required to create two simulations. As in the papers above, the SPH modelling technique was used for the soft projectile. Contrastingly, the hard projectile was much simpler to model, with elastic material elements being employed. The good agreement achieved from both simulations can be seen in Figure 4.

4.2. Impact Simulation of Repaired Composites

4.2.1. Mechanical Testing

When considering the impact performance of repaired composite panels, it is also critical to consider their performance in other mechanical testing. This section gives a brief summary of some modelling work that has been performed to consider this. All of the cases discussed are relatively simple models, but the general conclusions drawn appear accurate and useful to apply when modelling repaired composite panels.
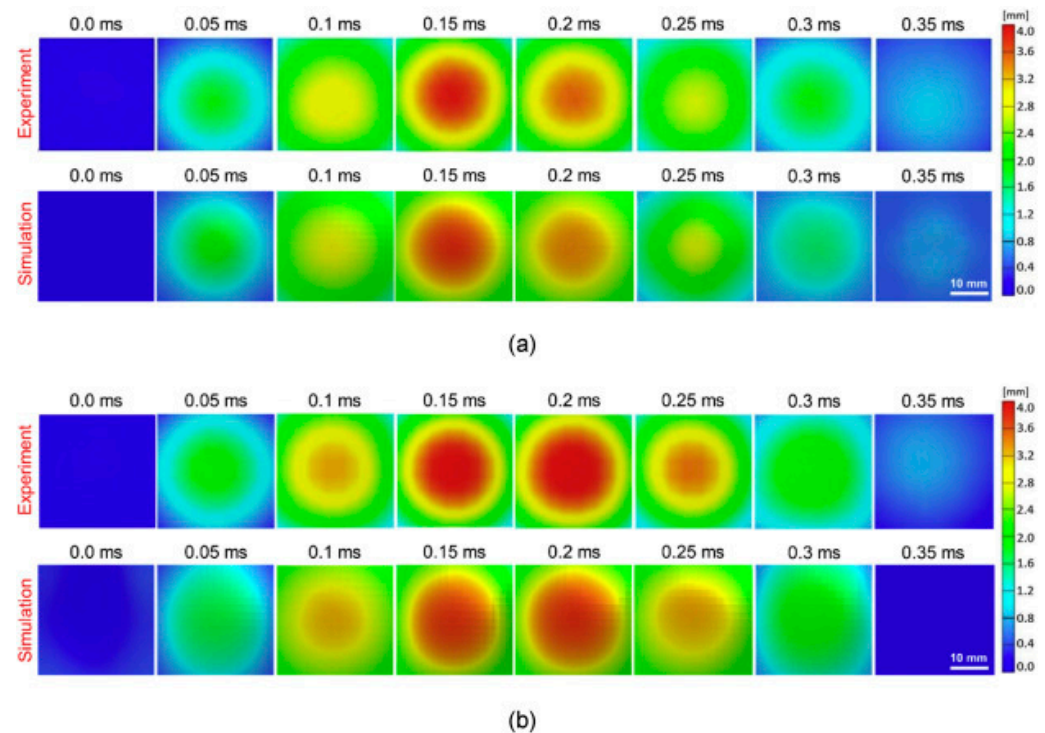
Figure 4. The out-of-plane displacement traces of high-velocity impacts on woven carbon-fibre/PEEK samples from experimental and numerical work for (**a**) a gelatine projectile, and (**b**) a HDPE projectile by Liu et al. [48].

The results from the work by Charalambides et al. [19] was then used by Charalambides et al. [49] with finite element analysis to derive the stress-versus-strain distribution in repair joints, to continue the research. For the model, sixteen rows of elements were used across the thickness of the parent composite, and one end of the joint was modelled as being clamped. Two material models were used for the adhesive: a simple linear elastic and a linear elastic-plastic. For the composite, linear elastic models were used throughout because the strains involved were low. There were also two different models used for the composite; the first represented the sixteen plies as a homogeneous orthotropic model, and the second modelled each ply individually with properties determined by the fibre angle. The latter of these two was found to give more accurate failure predictions but was much more time consuming. As stated above, this is a relatively simple model, but the demonstration that modelling the individual plies is more accurate than modelling the composite as one solid block appears to be a useful and correct conclusion.

Dan et al. [50] carried out stress analysis and evaluated the strength of scarf adhesive joints subjected to static tensile loading using 3D finite element analysis. The results yielded imply that the maximum value of the maximum principal stress occurs at the edge of the interfaces and is lowest at a scarf angle of 60°. It was also observed that the singular stress at the edge of the interface decreases by increasing the Young's Modulus of the adhesive and decreasing the thickness of the adhesive layer. This suggests that the choice of adhesive is extremely important when repairing composite structures and should be optimised to improve the properties of the final material.

A ductile adhesive was simulated by Pinto et al. [15] using trapezoidal cohesive laws. Bonding laminating plies on the outer face or both sides of the repair joint and repairs without any patching were simulated using the final model developed. Using different scarf angles was also investigated, and it was observed that the peel stress distributions were higher but more uniform for larger angles. Shear stress distributions were also seen to be more uniform for larger angles but were actually slightly lower in comparison to smaller angles. Pinto et al. [15] concluded that reducing the scarf angle increased the improvement

in strength, and therefore it is recommended to use smaller angles. Using patches on both sides of the scarf repairs was seen to have a strength of 70% that of the undamaged sample, whereas it was 50% for those without the patching. Therefore, adding patches was said to improve the repair efficiency, and, even if only applying on one side of the joint is possible, it is recommended. Although the results found seem viable, the specific values found may not be entirely accurate as this model does not take into account the inter- and intralaminar damage near the scarf join, focusing only on the adhesive failure. These failure mechanisms are likely to occur experimentally and so should be considered when modelling, but the extent to which excluding these affects the results found is unknown.

Gunnion et al. [51] varied the scarf angle, adhesive thickness, ply thickness, laminate thickness, over-laminate thickness, and lay-up sequence to investigate how each affected the peak stresses and stress distribution in the results from the model. It was observed that the stacking sequence greatly affected the peel and shear stresses of the sample, with peak values of 820% and 240% of the averages, respectively. Gunnion et al. [51] also stated that the stresses were very sensitive to the adhesive thickness, with a thicker adhesive causing a higher value of both peel and shear peak stresses. However, the average values of both stresses were concluded to be unaffected by the adhesive thickness. Contrastingly to Pinto et al. [15], the results found by Gunnion et al. [51] clearly showed that both the peel and shear stresses increased significantly with increasing scarf angles. Considering an over-laminate on the joint, it was concluded that the average shear and peel stresses decreased with an increase in the patch stiffness, and the peak values significantly decreased. This aligns with the conclusion of Pinto et al. [15] who stated that adding patches on either side of the repair improves the joint efficiency. It is important to note that both of these models have not been compared to experimental work performed by the authors, which may suggest limitations to the findings. However, when comparing to the relevant literature, the authors stated good agreement, so there is potential that the trends observed are accurate.

4.2.2. Low Velocity

Simulating a low-velocity impact of a scarf repair with a cohesive zone model based on Dugdale–Barenblatt model, Liu et al. [24] obtained results that implied that the finite element model used can simulate the damage propagation for composites with scarf repairs that are impacted. Experimental data, discussed in Section 3.3.1, was used to validate the model. From the model, it was seen that, when the impact energy increased to 10 J, composite intralaminar damage grew but adhesive shear fracture no longer did, which is a significant finding because the adhesive shear fracture was seen to be a major failure mode for the other impact energies simulated.

Cheng et al. [52] considered the effect that the stacking sequence and rotation angle of the scarf repair have on the impact performance. Fibre breakage and matrix cracking were modelled using 3D Hashin criteria, whilst in- and out-of-plane shear damage was found using maximum strain criteria. The final composite damage considered in this model was interface delamination, which was achieved through the use of cohesive elements. This finite element analysis model was found to have good agreement with experimental results, with a relative error of 8.2% between their average delamination areas. Three different scarf lay-ups were considered, along with a sequence of the same order as the parent material: the original lay-up was $[45/0_2/-45/90/45/0_2/-45/0]_S$; sequence 1 was $[0/-45/0_2/45/90/-45/0_2/45]_S$; sequence 2 was $[0_5/90/-45/45/-45/45]_S$; and sequence 3 was $[45/-45/45/-45/90/0_5]_S$. It was found that sequence 2 had the smallest delamination and adhesive damage areas, whilst sequence 3 had the largest adhesive damage area. Furthermore, sequence 1 was the most similar lay-up to the original lay-up of the parent material, but there was a difference between the total damage in the original patch and the one made with sequence 1. This demonstrates that a small change in the stacking sequence causes a change in the impact performance of the scarf repair. Ten rotation angles—$\pm3°$, $\pm5°$, $\pm7°$, $\pm9°$, and $\pm11°$—were simulated. From the results, it was noted that the patch rotation has an effect on the delamination damage, with a positive rotation

angle having a bigger effect than the negative angles. Finally, it is said that adjusting the rotation angle affects the overall performance of the scarf repair more so than changes in the stacking sequence.

A similar model was utilised by Cheng et al. [53] to consider the effect that scarf angle, adhesive thickness, and patch off-axis angle have on the overall repair performance. Additionally, the adhesive was modelled using a plastic model based on experimentation of the specific adhesive. Comparing the model results to experimental data, it was decided that the impact behaviour was predicted to a suitable accuracy. Firstly, the scarf angle was considered, with four angles from 5° to 8° being simulated. Both 7° and 8° had minimal delamination in the parent material, but 5° and 6° gave better tensile and compressive strength. Of these, 6° gives the least adherend delamination; however, 7° and 8° scarf angles are still recommended. Secondly, five adhesive thickness values were modelled between 0.1 and 0.25 mm, with results implying that thickness values within the range of 0.15 to 0.25 mm gave both better tensile and compressive strengths as well as better impact performance. Finally, eight angles between 0° and 180° were simulated for the patch off-axis angle. The maximum ultimate impact force was seen at a value of 0°, and the minimum occurred at 10°, suggesting that the patch off-axis angle has a notable effect on the impact performance. To reduce the damage to both the adhesive and adherend, an angle between 135° and 160° is recommended.

Tie et al. [29] used a continuum damage mechanics model, based on 3D Hashin failure criteria, and a cohesive zone model to investigate the effect of patch size and shape on the effectiveness of the repair. Five patch shapes were modelled: circle, square, rhombus, hexagon, and octagon, and it was seen that the initiation of damage happens at almost the same time for each sample. Additionally, the circular patch had the minimum impact force variation, meaning less impact energy was absorbed. Therefore, it was the patch shape with the best performance, and the rhombus was seen to have the worst performance. To consider the effect of patch size on the repair performance, circular patches with radii of 1.5, 2, 2.25, 2.5, 2.75, 3, and 3.5 times that of the hole radius were modelled. The smallest patch was found to have the worst performance, absorbing the most impact energy and having the largest damage area of all the modelled samples. All the other patch sizes were difficult to separate from the history curves alone, due to having such similar values. However, looking at the specific values of delamination area and energy absorption, it was seen that a circular patch with a radius of 2.5 that of the hole had the lowest values for both. This implies that the best repair performance is achieved with a circular patch that has a radius 2.5 times the size of the hole radius.

4.2.3. High Velocity

Kim et al. [32] modelled high-velocity impact testing of scarf-repaired composites using a finite element model. To minimise computational time and avoid shear locking, eight-node solid elements were used throughout the model apart from between the two adherends. Here, six-node solid elements were used instead, to prevent high aspect ratio and skew. For the adhesive itself, eight-node cohesive elements were utilised, allowing damage through the bond to be simulated. The second failure mode considered by this model was delamination, which was monitored implementing surface-based cohesive behaviour at the interfaces between layers. This model was seen to have good agreement with the experimental results obtained, meaning it could be used to investigate three damage scenarios: composite damage, adhesive damage, and a combination of the two. From this modelling, it was concluded that delamination reduces the extent to which adhesive disbonding occurs and that this is, in part, due to that fact that energy is dissipated by the delamination damage. However, this model does not account for intralaminar damage, which could mean that the conclusions drawn are be flawed, although the extent to which this exclusion affects the results is unknown.

Jiang et al. [54] used a continuum damage model with a modified 3D Hashin failure criteria, combined with a linear-exponential law, to predict the tensile softening processes,

and an exponential law, to predict the compressive softening processes of patch- and scarf-repaired composite materials. Comparisons with experimental data allowed optimisation of the model variables, such as mesh size, with good agreement being achieved. The composites simulated were repaired with a number of configurations, including a double-patch repair and a combination of both scarf and patched repair. The repair with the best performance was seen to be a scarf repair combined with a double-patch repair, with the largest difference between initial and residual velocities at a value of 48.3%. In general, combined repairs were concluded to have better perforation resistance capabilities, with ballistic limit velocities of over 80 m/s in comparison to below 55 m/s for composite repaired using a singular patch. The final observations made from this model were that the energy absorption almost increases with higher initial velocities, and moving the impact further from the repair site leads to a decrease in the average energy absorption.

4.3. Modelling Summary

Table 1 below gives the details of the models used in each numerical simulation scenario discussed above, allowing for a comparison between each technique used.

Table 1. Summary of modelling techniques implemented by references discussed above.

Model	Composite Panel Intralaminar	Composite Panel Interlaminar	Adhesive	Soft Impactor	Agreement
Pristine panels—hard impact					
Clark [34]	Predicts blocked damage in line with fibre direction of bottom ply at each interface		-	-	Predicts directions accurately but not delamination shapes
Topac et al. [9]	LaRC04 failure criterion	Cohesive zone model	-	-	Predicts the correct type of failure but otherwise does not match with experimental results
Ullah et al. [10]	Cohesive zone model implemented for both inter- and intralaminar damage		-	-	Predicts force time traces relatively well but too high for peak force value
Bouvet et al. [35]	Modified 2D Hashin criteria	Cohesive zone model	-	-	Predicts delamination shapes and areas well
Iannucci et al. [36,37]	Unconventional thermodynamic maximum energy dissipation approach		-	-	Predicts rear fibre breakage well but not as accurate for the force time traces
Xin et al. [39]	Quadratic stress-based failure criteria	Cohesive zone model with fracture energy approach	-	-	Predicts rear fibre breakage and force displacement traces relatively well but peak load too high
Ansari et al. [40]	Modified 3D Hashin criteria		-	-	Predicts residual velocity relatively well
Pham et al. [41]	General 3D maximum stress failure criterion	Cohesive zone model	-	-	Predicts damage orientation and initial stress–strain relationship well
Li et al. [45]	Modified Chang-Chang failure criteria	Griffith criterion	-	-	Predicts delamination size and shape, force time, and displacement time traces well

Table 1. *Cont.*

Model	Composite Panel		Adhesive	Soft Impactor	Agreement
	Intralaminar	Interlaminar			
Pristine panels—soft impact					
Johnson et al. [42,43]	Elastic or elastic-plastic damage mechanics model	Elastic damaging interface stress-displacement model	-	SPH method	Predicts the pressure in the soft projectile over time and damage relatively well
Nishikawa et al. [44]	Modified Chang-Chang failure criteria		-	Lagrange multiplier method	Predicts the force time traces well
Liu et al. [46–48]	2D Hashin criteria	Cohesive zone model	-	SPH method	Predicts displacement and rear face damage well
Repaired panels—general mechanical testing					
Charalambides et al. [49]	Modelling as one block vs. individual plies, thermal and hygrothermal expansion coefficients added to FEA model		Linear elastic vs. linear elastic-plastic	-	Predicts crack location well, modelling individual plies gave more accurate results and both adhesive models gave similar outputs
Dan et al. [50]	2D and 3D finite element method, with material treated as elastic		Bi-linear material model	-	Predicts strain through adhesive well
Pinto et al. [15]	Interlaminar and intralaminar failure near the scarf not considered		Trapezoidal cohesive zone model	-	No experimental work to verify, but agrees well with literature
Gunnion et al. [51]	Parametric FEA model		Linearity assumed	-	No experimental work to verify, but agrees well with literature
Repaired panels—low-velocity impact					
Liu et al. [24]	3D Hashin criteria	Yeh delamination failure criterion	Bi-linear cohesive zone model	-	Predicts adhesive damage and delamination area relatively well
Cheng et al. [52,53]	3D Hashin criteria	Cohesive zone model	Ductile damage criterion	-	Relative error of 8.2% in delamination area between model and experiments
Tie et al. [29]	3D Hashin criteria	Cohesive zone model	Quadratic separation law	-	Predicts load time traces well, not as accurate in predicting damage area
Repaired panels—high-velocity impact					
Kim et al. [32]	Intralaminar damage not considered	Cohesive zone model	Bi-linear traction separation law	-	Predicts load time traces well, not as accurate in predicting damage area
Jiang et al. [54]	Modified 3D Hashin criteria	Exponential softening law	Triangle traction separation law	-	Predicts rear face damage well

In general, the most common modelling techniques used for predicting intralaminar and interlaminar damage are 2D Hashin, 3D Hashin, or Chang-Chang criteria and a cohesive zone model, respectively. There are several techniques used to model the adhesive in the repaired panels, with the majority implementing a version of the cohesive zone model or a separation law. For the soft projectiles, the SPH method was most commonly used, and, where it was not used, an alternative Lagrangian method was used instead. The SPH modelling technique is a mesh-free Langrangian model, with the removal of the

mesh allowing for the deformation of the soft projectile to be more accurately predicted. The need for this is shown by Heimbs et al. [55] who compared Langrangian and Eulerian models, both of which include meshing, and saw an overprediction of the contact force upon impact of 11% and 5%, respectively. Having said this, relatively good agreement was still seen using both of these methods.

Shao et al. [56] compared the three modelling techniques used for predicting intralaminar damage. It was found that, including the effect on the damage within the matrix from the normal stress that acts through the thickness of the composite, two of the models gave better results and aligned more closely with those obtained experimentally. Both the 3D Hashin criteria and Chang-Chang criteria include this, but the 2D Hashin does not, highlighting the biggest drawback of the latter. Between the other two techniques, the 3D Hashin criteria gave slightly more accurate results. However, as can be seen in Figure 5 below, there is minimal difference, and all three techniques perform worse at a higher impact energy.
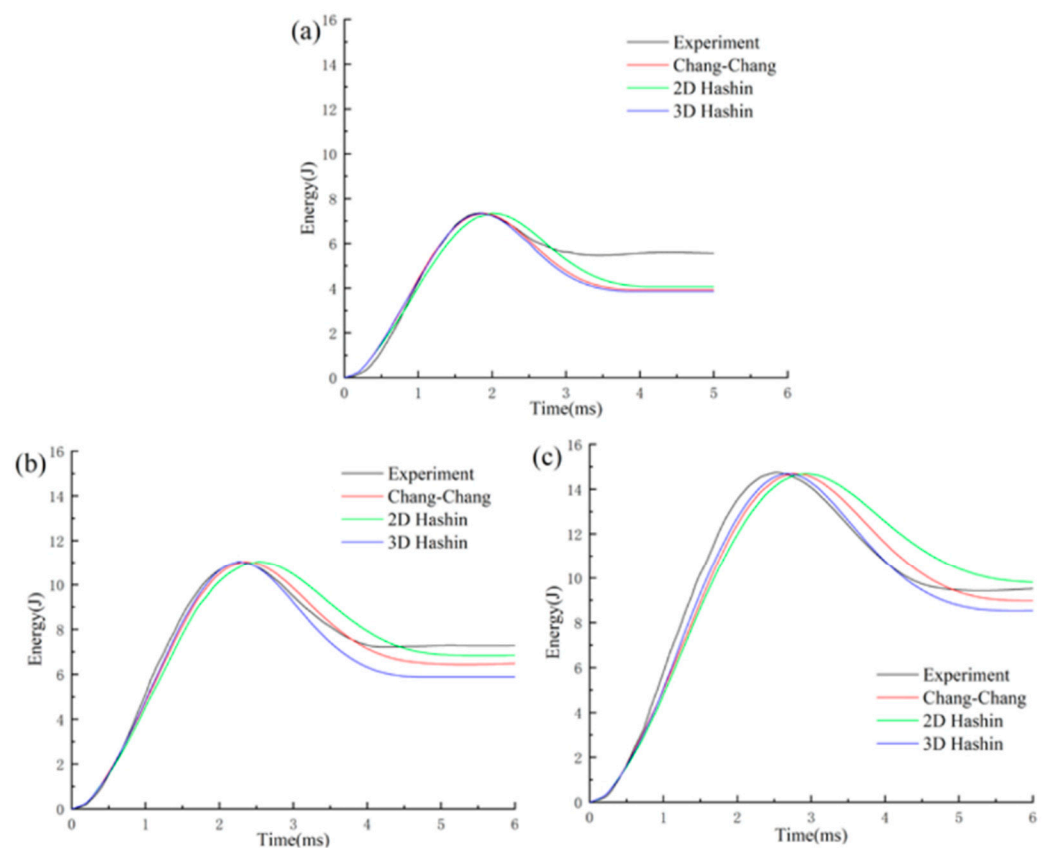

Figure 5. Comparison of time energy traces for 2D Hashin, 3D Hashin, and Chang-Chang failure criteria to experimental results at impact energies of (**a**) 7.35 J, (**b**) 11.03 J, and (**c**) 14.70 J [56].

5. Discussions

5.1. Hard Impact on Pristine Samples

Liu et al. [6] carried out research using unidirectional carbon-fibre-reinforced epoxy composites to assess the impact response at low velocities. Failure modes recorded in testing showed that fibre-dominated and matrix-dominated damage were accounted for in the intralaminar model. It was also seen that delamination was the most prominent failure mode, and there was no fibre breakage, which contrasts to soft impacts where large amounts of fibre breakage were observed. It also differs from the results found by Sjogren et al. [7], who found fibre breakage to be present in the low-velocity impacted samples but only within the delamination area. Furthermore, considering the initiation and evolution of damage during an impact event, Topac et al. [9] found that matrix cracking starts first

and then leads to delaminations. Additionally, it was observed that, where matrix cracking occurred on both sides of the panel, one crack clearly initiated first. Liu et al. [6] saw a visible indentation left on the test sample with a diameter of around 5 mm, which was accurately simulated using a finite element analysis model. This demonstrates the accuracy achievable with a simulation, meaning producing a model alongside testing in the earlier stages of the research project can save time and expense in later testing. Clark et al. [8] furthered the research on low-velocity impact by considering the fatigue strength after an impact occurred, demonstrating that, even on samples with small indentation and damage from impact, failure from fatigue is much more likely than for a pristine sample. This shows that, even if an impact does not cause failure of the component initially, when the aircraft is in flight the fatigue is likely to result in a failure.

For hard-impact testing, considering both low and medium velocities, which are defined as velocities considerably less than 75 m/s, the research of Olsson [11] states that interlaminar shear stresses are the primary cause of delamination in impacts. The tested composite was made from conventional unidirectional tape prepregs. This means that the specific properties of the delamination, including the observed peanut shape, may not apply to woven carbon epoxy composites or might only be relevant for the specific fibre and epoxy tested. Therefore, these properties should be tested for other lay-ups and materials to see how differently they compare.

Modelling the hard impact testing with finite element analysis is an area of interest because it allows for predictions to be made before carrying out expensive testing. However, the models must be reliable and give accurate results to be of any use. Bouvet et al. [35] state that the key point for an impact model is the interaction between intralaminar damage, namely matrix cracks and fibre failure, and interlaminar damage, namely delamination. This statement implies that the model needs to be thoroughly tested with different interactions and material properties to find the most reliable and suitable simulation. This is supported by Iannucci et al. [38] who concluded that there are many properties and constants that need to be determined accurately for their model to be reliable. Another issue encountered with modelling these impacts was seen by Clark [34], where most of the different layups had either good or excellent agreement with the experimental results, but one case had some disagreement. Admittedly, the model by Clark [34] is simple, and this is likely what led to the disparity. However, it does highlight that, even if a model is suitable for a certain lay-up, it may not be as agreeable for others.

5.2. Soft Impact on Pristine Samples

From the experimental testing carried out by Hou et al. [12] and Pernas-Sanchez et al. [13], it is implied that the toughness of both the fibre and resin and the thickness of the composite have significant effects on the overall performance of the material under soft impact.

In continuation, the numerical modelling carried out by Johnson et al. [42,43] and Nishikawa et al. [44] shows that simulated results can be produced to have good agreement with experimental results. Different modelling techniques can be implemented for the same problem, with Johnson et al. [42] investigating an interacting particle mesh type for the projectile, giving promising results that could be developed further by considering other failure modes and varying material properties to check agreement in other areas. Meanwhile, Nishikawa et al. [44] used a different Lagrangian model and still obtained good agreement. Their model aimed to find how the fibre breakage mode affects the ballistic limit, and they saw that changing the voltage causes the failure mode to transition to a different combination. These simulation results act as good indicators of properties and conditions to adjust when carrying out experimental testing in the future.

5.3. Repaired Composites

The change of failure mode seen by Charalambides et al. [19] when varying the water saturation level implies that this can be controlled to give the most suitable failure path for

the location of the repair to improve the repair efficiency. Further research could be carried out by investigating different periods of water immersion to those used by Charalambides et al. [19] as well as testing a variety of adhesives and curing techniques. In continuation, the finite element analysis carried out by Charalambides et al. [49] proved to be largely successful, demonstrating that modelling the composite as individual plies rather than one block gives a model that more closely aligns with experimental results.

Both Kumar et al. [20] and Dan et al. [50] carried out research that considered the effects of the scarf angle on the performance of the repaired sample. From the results found, it was concluded that the scarf angle affects the tensile strength and maximum principal stress, which implies this angle is closely related to the mechanical performance of the repaired material. To minimise the reduction in tensile strength of repairing the composite, Kumar et al. [20] found small angles (around $1°$) to be most suitable. In contrast, an angle of $60°$ is recommended by Dan et al. [50] to reduce the maximum principal stress. These papers imply that a compromise between tensile strength and minimising the maximum principal stress is required when choosing the scarf angle. Li et al. [21] also considered the scarf angle, concluding that large values improve the shear strength but decrease the ultimate failure load. This further shows the point that a compromise between repair performance parameters is required when choosing a scarf angle.

The performance in impact testing, considered by Liu et al. [23] and Liu et al. [28], implies that the join is the weakest section of the repaired composite but that there is an impact energy, below which, the sample exhibits the same failure modes as a pristine material. Overall, this research implies that the adhesive joint properties require testing and optimising to raise the impact energy value and improve the residual strength at the joint edges.

A lot of research has been carried out in modelling repair performance, with Pinto et al. [15] and Gunnion et al. [51] both considering the peel and shear stresses in a repair joint. Although slightly different results were found, both sets of research came to the same two conclusions that a smaller scarf angle gives a better strength performance and adding patches to either side of the repair joint improves the joint efficiency. Both models were seen to have good agreement with experimental results. However, in both cases there was no comparison to experimental testing performed by the authors, but instead a comparison to other literature. For this reason, the conclusions could be explored further using modelling in conjunction with experimental work.

6. Conclusions

The primary focus of this review is the impact testing on pristine and repaired composites. An investigation into the comparison between hard and soft impact testing has also been explored. The main difference observed between these two types of impact was that permanent indentations are left on the impacted face for hard impacts but not for softer impacts. This is because the soft projectiles deform around the sample rather than indent it. Modelling this phenomenon is quite challenging, with a few different techniques being available. In general, modelling impact response is challenging due to the reliance on many constants that must be found accurately to ensure a reliable result from the simulation.

The damage observed on the composite samples tested is often localised, meaning that a repair could potentially be possible if the suitability of the adhesive is to a high enough standard to meet safety requirements in the aerospace industry. The repair of composite materials in aircraft is an area that also requires more research and testing to improve the performance and strengthen the adhesive joint itself. This is because the life of the components of an aircraft is less than the aircraft itself. However, replacing entire panels would be extremely expensive and time-consuming, meaning that an effective repair technique is required for composite materials to be a viable option in aerostructures. From the research discussed in this paper, the thickness of the adhesive, the scarf angle, and other parameters can be adjusted to give the required performance.

Further research into the performance of repaired composite structures is required, specifically the performance under soft impact testing as this has not been explored in detail. Additionally, other areas that could be investigated are the performance of repairs under high-velocity impacts and considering a larger range of values for the repair variables already considered, such as a wider range of impact locations and patch sizes.

Author Contributions: Conceptualization, Z.E.C.H. and H.L.; investigation, Z.E.C.H.; resources, Z.E.C.H.; data curation, Z.E.C.H.; writing—original draft preparation, Z.E.C.H.; writing—review and editing, J.L., R.A.B., H.L. and J.P.D.; visualization, Z.E.C.H. and J.L.; supervision, J.P.D.; project administration, H.L. All authors have read and agreed to the published version of the manuscript.

Data Availability Statement: No new data were created or analyzed in this study. Data sharing is not applicable to this article.

Conflicts of Interest: The authors declare no conflict of interest.

References

1. Van Minh, P.; Nguyen, D.T.; Doan, L.T.; Nguyen, D.V.; Duong, T.V. Numerical investigation on static bending and free vibration responses of two-layer variable thickness plates with shear connectors. *Iran J. Sci. Technol. Trans. Mech. Eng.* **2022**, *46*, 1047–1065. [CrossRef]
2. Nguyen, D.T.; Van Minh, P.; Hoang, C.P.; Tam, T.D.; Nhung, N.T.C.; Nguyen, T.D. Bending of symmetric sandwich FGM beams with shear connectors. *Math Probl. Eng.* **2021**, *2021*, 7596300. [CrossRef]
3. Nguyen, T.C.; Van Thom, D.; Pham, C.H.; Zenkour, A.M.; Doan, D.H.; Van Minh, P. Finite element modelling of the bending and vibration behaviour of three-layer composite plates with a crack in the core layer. *Compos. Struct.* **2023**, *305*, 116529. [CrossRef]
4. Nguyen, T.D.; Van Minh, P.; Hoang, M.H.; Dao, M.T. The third-order shear deformation theory for modelling the static bending and dynamic responses of piezoelectric bidirectional functionally graded plates. *Adv. Mater Sci. Eng.* **2021**, *2021*, 5520240. [CrossRef]
5. Nam, V.H.; Nguyen, N.H.; Pham, V.V.; Khoa, D.N.; Van Thom, D.; Van Minh, P. A new efficient modified first-order shear model for static bending and vibration behaviours of two-layer composite plate. *Adv. Civ. Eng.* **2019**, *2019*, 2385106. [CrossRef]
6. Liu, H.; Falzon, B.G.; Tan, W. Experimental and numerical studies on the impact response of damage-tolerant hybrid unidirectional/woven carbon-fibre reinforced composite laminates. *Compos. Part B* **2018**, *136*, 101–118. [CrossRef]
7. Sjogren, A.; Krasnikovs, A.; Varna, J. Experimental determination of elastic properties of impact damage in carbon fibre/epoxy laminates. *Compos. Part A* **2001**, *32*, 1237–1242. [CrossRef]
8. Clark, G.; Van Blaricum, T.J. Load spectrum modification effects on fatigue of impact-damaged carbon fibre composite coupons. *Composites* **1987**, *18*, 243–251. [CrossRef]
9. Topac, O.T.; Gozluklu, B.; Gurses, E.; Coker, D. Experimental and computational study of the damage process in CFRP composite beams under low-velocity impact. *Compos. Part A* **2017**, *92*, 167–182. [CrossRef]
10. Ullah, H.; Harland, A.R.; Silberschmidt, V.V. Damage and fracture in carbon fabric reinforced composites under impact bending. *Compos. Struct.* **2013**, *101*, 144–156. [CrossRef]
11. Olsson, R. Low-and medium-velocity impact as a cause of failure in polymer matrix composites. In *Failure Mechanisms in Polymer Matrix Composites*; Woodhead Publishing: Sawston, UK, 2012; pp. 53–78. [CrossRef]
12. Hou, J.P.; Ruiz, C. Soft body impact on laminated composite materials. *Compos. Part A* **2007**, *38*, 505–515. [CrossRef]
13. Pernas-Sanchez, J.; Artero-Guerrero, J.A.; Varas, D.; Lopez-Puente, J. Experimental analysis of ice sphere impacts on unidirectional carbon/epoxy laminates. *Int. J. Impact Eng.* **2016**, *96*, 1–10. [CrossRef]
14. Kimiaeifar, A.; Toft, H.; Lund, E.; Thomsen, O.T.; Sorensen, J.D. Reliability analysis of adhesive bonded scarf joints. *Eng. Struct.* **2012**, *35*, 281–287. [CrossRef]
15. Pinto, A.M.; Campilho, R.D.; de Moura, M.F.; Mendes, I.R. Numerical evaluation of three-dimensional scarf repairs in carbon-epoxy structures. *Int. J. Adhes. Adhes.* **2010**, *30*, 329–337. [CrossRef]
16. Katnam, K.B.; Da Silva, L.F.; Young, T.M. Bonded repair of composite aircraft structures: A review of scientific challenges and opportunities. *Prog. Aerosp. Sci.* **2013**, *61*, 26–42. [CrossRef]
17. Demiral, M.; Abbassi, F.; Saracyakupoglu, T.; Habibi, M. Damage analysis of a CFRP cross-ply laminate subjected to abrasive water jet cutting. *Alex. Eng. J.* **2022**, *61*, 7669–7684. [CrossRef]

18. Preau, M.; Hubert, P. Processing of co-bonded scarf repairs: Void reduction strategies and influence on strength recovery. *Compos. Part A* **2016**, *84*, 236–245. [CrossRef]

19. Charalambides, M.N.; Hardouin, R.; Kinloch, A.J.; Matthews, F.L. Adhesively-bonded repairs to fibre-composite materials I: Experimental. *Compos. Part A* **1998**, *29*, 1371–1381. [CrossRef]

20. Kumar, S.B.; Sridhar, I.; Sivashanker, S.; Osiyemi, S.O.; Bag, A. Tensile failure of adhesively bonded CFRP composite scarf joints. *Mater. Sci. Eng. B* **2006**, *132*, 113–120. [CrossRef]

21. Li, J.; Yan, Y.; Zhang, T.; Liang, Z. Experimental study of adhesively bonded CFRP joints subjected to tensile loads. *Int. J. Adhes. Adhes.* **2015**, *57*, 95–104. [CrossRef]

22. Slattery, P.G.; McCarthy, C.T.; O'Higgins, R.M. Assessment of residual strength of repaired solid laminate composite materials through mechanical testing. *Compos. Struct.* **2016**, *84*, 236–245. [CrossRef]

23. Liu, B.; Xu, F.; Qin, J.; Lu, Z. Study on impact damage mechanisms and TAI capacity for the composite scarf repair of the primary load-bearing level. *Compos. Struct.* **2017**, *181*, 183–193. [CrossRef]

24. Liu, B.; Han, Q.; Zhong, X.; Lu, Z. The impact damage and residual load capacity of composite stepped bonding repairs and joints. *Compos. Part B* **2019**, *158*, 339–351. [CrossRef]

25. Atas, C.; Akgun, Y.; Dagdelen, O.; Icten, B.M.; Sarikanat, M. An experimental investigation on low velocity impact response of composite plates repaired by VARIM and hand lay-up process. *Compos. Struct.* **2011**, *93*, 1178–1186. [CrossRef]

26. Li, H.C.H.; Mitrevski, T.; Herszberg, I. Impact on bonded repairs to CFRP laminates under load. In Proceedings of the 25th International Congress of the Aeronautical Sciences, Hamburg, Germany, 3–8 September 2006.

27. Herszberg, I.; Feih, S.; Gunnion, A.J.; Li, H.C.H. Impact damage tolerance of tension loaded bonded scarf repairs to CFRP laminates. In Proceedings of the 16th International Conference on Composite Materials, Kyoto, Japan, 8–13 July 2007.

28. Liu, S.F.; Cheng, X.Q.; Xu, Y.Y.; Bao, J.W.; Guo, X. Study on impact performances of scarf-repaired carbon fibre reinforced polymer laminates. *J. Reinf. Plast. Compos.* **2015**, *34*, 60–71. [CrossRef]

29. Tie, Y.; Hou, Y.; Li, C.; Zhou, X.; Sapanathan, T.; Rachik, M. An insight into the low-velocity impact behaviour of patch repaired CFRP laminates using numerical and experimental approaches. *Compos. Struct.* **2018**, *190*, 179–188. [CrossRef]

30. Coelho, S.R.M.; Reis, P.N.B.; Ferreira, J.A.M.; Pereira, A.M. Effects of external patch configuration on repaired composite laminates subjected to multi-impacts. *Compos. Struct.* **2017**, *168*, 259–265. [CrossRef]

31. Hou, Y.; Tie, Y.; Li, C.; Sapanathan, T.; Rachik, M. Low-velocity impact behaviours of repaired CFRP laminates: Effect of impact location and external patch configurations. *Compos. Part B* **2019**, *163*, 669–680. [CrossRef]

32. Kim, M.K.; Elder, D.J.; Wang, C.H.; Feih, S. Interaction of laminate damage and adhesive disbonding in composite scarf joints subjected to combined in-plane loading and impact. *Compos. Struct.* **2012**, *94*, 945–953. [CrossRef]

33. Balaganesan, G.; Khan, V.C. Energy absorption of repaired composite laminates subjected to impact loading. *Compos. Part B* **2016**, *98*, 39–48. [CrossRef]

34. Clark, G. Modelling of impact damage in composite laminates. *Composites* **1989**, *20*, 209–214. [CrossRef]

35. Bouvet, C.; Rivallant, S.; Barrau, J.J. Low velocity impact modelling in composite laminates capturing permanent indentation. *Compos. Sci. Technol.* **2012**, *72*, 1977–1988. [CrossRef]

36. Iannucci, L. Progressive failure modelling of woven carbon composite under impact. *Int. J. Impact Eng.* **2006**, *32*, 1013–1043. [CrossRef]

37. Iannucci, L.; Willows, M.L. An energy based damage mechanics approach to modelling impact onto woven composite materials: Part, I. Numerical models. *Compos. Part A* **2007**, *37*, 2041–2056. [CrossRef]

38. Iannucci, L.; Willows, M.L. An energy based damage mechanics approach to modelling impact onto woven composite materials: Part II. Experimental and numerical results. *Compos. Part A* **2007**, *38*, 540–554. [CrossRef]

39. Xin, S.H.; Wen, H.M. A progressive damage model for fibre reinforced plastic composites subjected to impact loading. *Int. J. Impact. Eng.* **2015**, *75*, 40–52. [CrossRef]

40. Ansari, M.M.; Chakrabarti, A. Impact behaviour of FRP composite plate under low to hyper velocity impact. *Compos. Part B* **2016**, *95*, 462–474. [CrossRef]

41. Pham, D.C.; Lua, J.; Sun, H.; Zhang, D. A three-dimensional progressive damage model for drop-weight impact and compression after impact. *J. Compos. Mater.* **2018**, *54*, 449–462. [CrossRef]

42. Johnson, A.F.; Holzapfel, M. Modelling soft body impact on composite structures. *Compos. Struct.* **2003**, *61*, 103–113. [CrossRef]

43. Johnson, A.F.; Holzapfel, M. Numerical prediction of damage in composite structures from soft body impacts. *J. Mater. Sci.* **2006**, *41*, 6622–6630. [CrossRef]

44. Nishikawa, M.; Hemmi, K.; Takeda, N. Finite-element simulation for modelling composite plates subjected to soft-body, high-velocity impact for application to bird-strike problem of composite fan blades. *Compos. Struct.* **2011**, *93*, 1416–1423. [CrossRef]

45. Li, C.F.; Hu, N.; Cheng, J.G.; Fukunaga, H.; Sekine, H. Low-velocity impact-induced damage of continuous fiber-reinforced composite laminates. Part II. Verification and numerical investigation. *Compos. Part A* **2002**, *33*, 1063–1072. [CrossRef]

46. Liu, H.; Liu, J.; Kaboglu, C.; Chai, H.; Kong, X.; Blackman, B.R.K.; Kinloch, A.J.; Dear, J.P. Experimental and numerical studies on the behaviour of fibre-reinforced composites subjected to soft impact loading. In Proceedings of the 3rd International Conference on Structural Integrity, Madeira, Portugal, 2–5 September 2019; pp. 992–1001. [CrossRef]

47. Liu, H.; Liu, J.; Kaboglu, C.; Zhou, J.; Kong, X.; Blackman, B.R.K.; Kinloch, A.J.; Dear, J.P. The behaviour of fibre-reinforced composites subjected to a soft impact-loading: An experimental and numerical study. *Eng. Fract. Anal.* **2020**, *111*, 104448. [CrossRef]

48. Liu, H.; Liu, J.; Ding, Y.; Zheng, J.; Luo, L.; Kong, X.; Zhou, J.; Blackman, B.R.K.; Kinloch, A.J.; Dear, J.P. Modelling the effect of projectile hardness on the impact response of a woven carbon-fibre reinforced thermoplastic-matrix composite. *Int. J. Lightweight Mater. Manuf.* **2020**, *3*, 403–415. [CrossRef]

49. Charalambides, M.N.; Kinloch, A.J.; Matthews, F.L. Adhesively-bonded repairs to fibre-composite materials II: Finite element modelling. *Compos. Part A* **1998**, *29*, 1383–1396. [CrossRef]

50. Dan, H.; Sawa, T.; Iwamoto, T.; Hirayama, Y. Stress analysis and strength evaluation of scarf adhesive joints subjected to static tensile loadings. *Int. J. Adhes. Adhes.* **2010**, *30*, 387–392. [CrossRef]

51. Gunnion, A.J.; Herszberg, I. Parametric study of scarf joints in composite structures. *Compos. Struct.* **2006**, *75*, 364–376. [CrossRef]

52. Cheng, X.; Du, X.; Zhang, J.; Zhang, J.; Guo, X.; Bao, J. Effects of stacking sequence and rotation angle of patch on low velocity impact performance of scarf repaired laminates. *Compos. Part B* **2018**, *133*, 78–85. [CrossRef]

53. Cheng, X.; Zhang, J.; Bao, J.; Zeng, B.; Cheng, Y.; Hu, R. Low-velocity impact performance and effect factor analysis of scarf-repaired composite laminates. *Int. J. Impact Eng.* **2018**, *111*, 85–93. [CrossRef]

54. Jiang, H.; Ren, Y.; Zhang, S.; Liu, Z.; Yu, G.; Xiang, J. Damage and perforation resistance behaviours induced by projectile impact load on bonding-patch repaired and scarf-patch repaired composite laminates. *Int. J. Damage Mech.* **2019**, *28*, 502–537. [CrossRef]

55. Heimbs, S.; Bergmann, T. High-velocity impact behaviour of prestressed composite plates under bird strike loading. *Int. J. Aerosp. Eng.* **2012**, *2012*, 372167. [CrossRef]

56. Shao, J.R.; Liu, N.; Zheng, Z.J. Numerical comparison between Hashin and Chang-Chang failure criteria in terms of inter-laminar damage behaviour of laminated composites. *Mater. Res. Express* **2021**, *8*, 085602. [CrossRef]